11th International Symposium on Magnetic Bearings
August 26-29, Nara, Japan

PARAMETERIZED ELECTROMECHANICAL MODEL FOR MAGNETIC BEARINGS WITH INDUCED CURRENTS

Virginie Kluyskens
Centre for Research in Mechatronics
Université Catholique de Louvain, Louvain-la-Neuve, Belgium
virginie.kluyskens@uclouvain.be
Bruno Dehez
Centre for Research in Mechatronics
Université Catholique de Louvain, Louvain-la-Neuve, Belgium
bruno.dehez@uclouvain.be

ABSTRACT

The purpose of this paper is to present a parameterized electromechanical model considering as well the electromagnetic nature of the forces acting inside a magnetic bearing as the general rotating machinery aspects, and their interactions. This model takes particularly the effect of induced currents into account. The inductive and resistive effects, as well as the skin effect taking place in the bearing are considered. The model is validated on an existing semi-passive magnetic bearing.

I. INTRODUCTION

Magnetic bearings can prove to be useful in various situations, like high-speed or vacuum applications where classical roller bearings reach their limits. These bearings can be classified into different categories: active, passive or semi-passive.

Good compromise between low cost and high performance can be achieved via a hybrid magnetic bearing [1]: some degrees of freedom being controlled, others not.

However, studies have shown the onset of unexpected vibrations on semi-passive magnetic bearings [2]. They are unexpected because they take place after critical speeds of the system have been passed, and they are not due to gyroscopic effects. To understand this phenomenon, we developed in [3] an electromechanical model based on the idea that the forces due to the interaction between the induced currents and the magnetic fields can be modeled by introducing damping into the mechanical equations governing the magnetic bearing motion. This model, whose principal lines are presented in this article, had already been validated in [3] on the basis of results obtained using finite element software on a simplified case modeled in 3D, and on experimental results for this simplified case.

The first aim of this developped electromechanical model was to fully understand and explain the observed unstable behavior. The second aim of this model is now to have a practical tool to design new stable magnetic bearings, or eventuelly to correct existing unstable magnetic bearings. With this model, this can be done on the basis of a few experimental measurements, or on the basis of a finite element model of the bearing. A macroscopic point of view is chosen on the electromagnetic phenomenon involved in the system, and there is no need to develop an often complex analytical solution for the magnetic and electric fields.
The objective of this paper is to present some refinements made on the previous electromechanical model [3]: the damping coefficient representing the forces due to induced currents is not considered as constant anymore, it depends on the inductive and the resistive behavior of the conducting piece where the induced currents take place. Furthermore, the skin effect is taken into account. And finally, a more advanced analysis of the stability conditions is made. It is shown that the model predicts stable and unstable speed ranges. This electromechanical model is validated on an existing semi-passive magnetic bearing (Fig.1).

Figure 1: Stator of semi-passive magnetic bearing

II. MODEL

Magnetic bearings are electromechanical systems with a strong interaction between the electromagnetic aspects and the mechanical aspects. Therefore it is important to take both aspects into account when modeling the behavior of a magnetic bearing.

First, a fast and general reminder of mechanical equations is exposed, showing that damping associated to rotating parts can generate an unstable behavior. Second, an electromechanical model is developed integrating as well the rotating modeling as the electromagnetic nature of the forces acting on a magnetic bearing.

2.1 Mechanical approach

When writing the mechanical equations of a system with a rotating shaft submitted to elastic and damping forces, it is important to look at the place where the damping takes place [4].

Let us name:

- c_r , the damping coefficient associated with rotating parts of the system;
- c_{nr} , the damping coefficient associated with non-rotating parts of the system;
- k, the stiffness coefficient of the elastic force;
- $x,y,$ the position of the rotor in the plane perpendicular to the rotation axis;
- $z=x+jy$, a complex notation used to express the position of the rotor and to write the equations of motion.

The equation of motion of point mass, weighing m, and attached to a mass less shaft is then:

$$m\ddot{z} + (c_{nr} + c_r)\dot{z} + (k - j\omega c_r) = 0 \qquad (1)$$

with ω the spin speed.

The solution of this equation can be written in the form:

$$\begin{cases} x = z_0 \exp(-\lambda_I t)\cos(\lambda_R t) \\ y = z_0 \exp(-\lambda_I t)\sin(\lambda_R t) \end{cases},$$

where λ_R and λ_I are the real and imaginary part of λ:

$$\lambda = \mp\frac{1}{\sqrt{2}}\sqrt{\Gamma + \sqrt{\Gamma^2 + \left(\frac{\omega c_r}{m}\right)^2}} + j\left(\frac{c_r + c_{nr}}{2m} \pm \frac{1}{\sqrt{2}}\sqrt{-\Gamma + \sqrt{\Gamma^2 + \left(\frac{\omega c_r}{m}\right)^2}}\right) \qquad (2)$$

with:

$$\Gamma = \frac{k}{m} - \frac{(c_{nr} + c_r)^2}{4m^2}.$$

The first solution corresponds to an always-damped backward whirl motion. It has a negative real part and an always positive imaginary part for λ.

The second solution corresponds to a forward whirl motion, it has a positive real part. It is only damped when the imaginary part of λ is negative, that is for a spin speed ω smaller than a limit spin speed ω_{lim} given by:

$$\omega_{lim} = \sqrt{\frac{k}{m}}\left(1 + \frac{c_{nr}}{c_r}\right) \qquad (3)$$

When the spin speed ω is bigger than ω_{lim}, the whirl motion is not damped anymore, but amplified, and the rotor undergoes an unstable behavior. When the spin speed increases beyond ω_{lim}, the rotor never goes back to a stable behavior. The more the ratio non-rotating over rotating damping is small, the more the limit spin speed is close to the critical speed.

2.2 Electromechanical approach

The electromechanical model presented in this section is based on the idea that the electromagnetic forces acting within a magnetic bearing can be modeled by mechanical components like springs and dampers. Indeed, on one hand, the reluctance forces can be modeled by stiffnesses, as they are proportional to the relative displacement. While, on the other hand, the Lorentz forces due to the interaction between induced currents, due to relative speed, and magnetic fields, can be modeled by introducing damping into the equations. According to the place where the eddy currents take place, they will be modeled by rotating damping (in the rotor) or by non-rotating damping (in the stator).

However, these Lorentz forces can not be modeled by simply replacing the rotating damping coefficient by an appropriate constant in equation (1). Indeed, when an electromotive force is induced on a conducting piece, the currents generated consequently are subjected to inductive end resistive effects. Since the Lorentz forces are proportional to the induced currents, and act in a direction determined by thesee induced currents, these forces are also subjected to these resistive and inductive effects. These effects will be felt on the orientation of the force: the induced currents have a phase shift in regard to the electromotive force function of the inductive and resistive effects. They will also have consequences on the norm of the force: the norm of these induced currents depends on the norm of the electromotive force trough the impedance, and then, trough the resistive and inductive effects.

In order to quantatively formalize these effects, we will first consider that:

- there are only eddy currents in the rotor;
- the resistive effects taking place in the rotor can be represented by a global resistance R;
- the inductive effects taking place can be represented by a global inductance L.

Next, we will introduce, as validated in [3], a complex rotating damping coefficient, $c_r = c_r' + j\,c_r''$, where:

- the real part, c_r', corresponding to the usual damping, can be related to the active power dissipated in the global resistance of the rotor;
- the imaginary part, c_r'', can be related to the reactive power produced by the global inductance of the rotor.

In a more rigorous way, this can be written as follow:

$$\begin{cases} \omega^2\, c_r' \propto e\, i \cos\theta \\ \omega^2\, c_r'' \propto e\, i \sin\theta \end{cases} \tag{4}$$

where θ, the phase shift between the electromotive force e and the induced current i, is given by:

$$\theta = \arctan\left(\omega L / R\right). \tag{5}$$

Considering the global impedance of the rotor, the relation between the induced currents i and the electromotive force e is:

$$i = \frac{e}{\sqrt{R^2 + \left(\omega L\right)^2}}. \tag{6}$$

Finally, assuming that the electromotive force e is proportional to the spin speed ω, equations (4) to (6) lead to:

$$\begin{cases} c_r' = c_r \cos\theta \\ c_r'' = c_r \sin\theta \end{cases}, \tag{7}$$

with:

$$c_r = c_m \frac{1}{\sqrt{R^2 + \left(\omega L\right)^2}}, \tag{8}$$

and c_m a proportionality constant.

In the particular case of a purely resistive conducting piece, where the inductance is zero, the damping coefficient is real and constant.

Finally, by substituting the complex damping coefficient into the equations of motion, we obtain:

$$\begin{pmatrix} m & 0 \\ 0 & m \end{pmatrix} \begin{pmatrix} \ddot{x} \\ \ddot{y} \end{pmatrix} = \begin{pmatrix} F_X \\ F_Y \end{pmatrix},$$

with:

$$\begin{pmatrix} F_X \\ F_Y \end{pmatrix} = \begin{pmatrix} -c_{nr} - c_r \cos\theta & c_r \sin\theta \\ -c_r \sin\theta & -c_{nr} - c_r \cos\theta \end{pmatrix} \begin{pmatrix} \dot{x} \\ \dot{y} \end{pmatrix} + \begin{pmatrix} -k_{nr} - c_r \omega \sin\theta & c_r \omega \cos\theta \\ -c_r \omega \cos\theta & -k_{nr} - c_r \omega \sin\theta \end{pmatrix} \begin{pmatrix} x \\ y \end{pmatrix}. \tag{9}$$

The limit spin speed is then equal to:

$$\omega_{lim} = \left(1 + \frac{c_{nr}}{c_r \cos\theta}\right)\left(\omega_{dyn} \pm \sqrt{\omega_{dyn}^2 + \omega_{cr}^2}\right), \tag{10}$$

with:

$$\begin{cases} \omega_{cr} = \sqrt{k/m} \\ \omega_{dyn} = c_{nr} \tan\theta / \left(2m\right) \end{cases}.$$

Let us note that equation (10) is a non-linear implicit equation since θ and c_r depends on ω in a non-linear way.

III. SKIN EFFECT

One more remark has to be done on this model: the impedance R and L used in the electromechanical model could be considered constant if the skin effect is not predominant, but usually magnetic bearings are made of massive parts and spin very fast, and then, skin effect is not negligible. The chosen law of evolution of the impedance with the frequency (spin speed in this case) is explained in [5]. The principle is based on a phenomenological approach. At low frequencies, the evolution law of the impedance is insignificant because skin depth is much higher than the characteristic dimensions of the system.

This low-frequency impedance is equal to:

$$Z_{lf} = R_{dc} + j\,\omega\left(L_0 + L_{int}\right), \tag{11}$$

with R_{dc} the direct current resistance, L_0 the inductance and L_{int} the internal inductance.

At high frequencies, the skin effect is predominant and the frequency evolution of the resistance and the inductance is well-known.

The high-frequency impedance is equal to:

$$Z_{hf} = R_{hf} + j\omega\left(L_0 + L_{hf}\right), \tag{12}$$

with

$$\begin{cases} R_{hf} = \alpha\sqrt{\omega} \\ L_{hf} = \alpha / \sqrt{\omega} \end{cases}.$$

At intermediate frequencies, it is supposed that the impedance is a combination of the low-frequency impedance (12) and the high frequency impedance (13) according to the following expression:

$$Z = \left(1 - g(\omega)\right) Z_{lf} + g(\omega) Z_{hf} \tag{13}$$

The weighing function $g(\omega)$ is equal to:

$$g(\omega) = 2/\pi \arctan\left(\gamma\,\omega + \beta\right) \tag{14}$$

IV. STABILITY ANALYSIS

First, let's take a look at the stability in equation (1). As said before there is one limit spin speed (3) beyond which there is no stable behavior possible anymore. The higher the rotating damping is, the lower the limit spin speed, as it is illustrated on figure 2. It can be observed that the rotating damping, which is a non conservative force, has a destabilizing role. When the ratio c_{nr} over c_r tend to infinity (c_r tends to zero), the limit spin speed tends to infinity too. But when c_r is not negligible, the behavior of the rotor is unstable beyond a finite limit spin speed ω_{lim}.

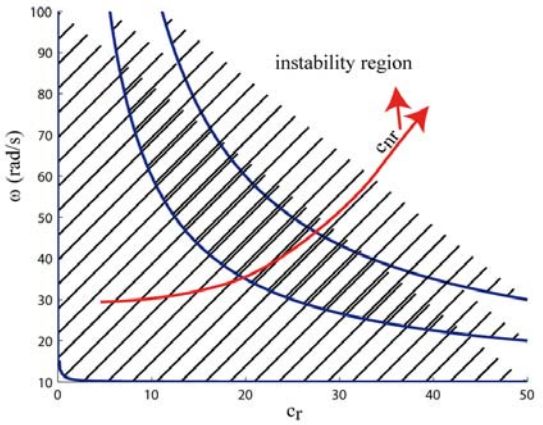

Figure 2: limit spin speed for mechanical model for a given set of parameters in function of the rotating (c_r) and the non-rotating (c_{nr}) damping

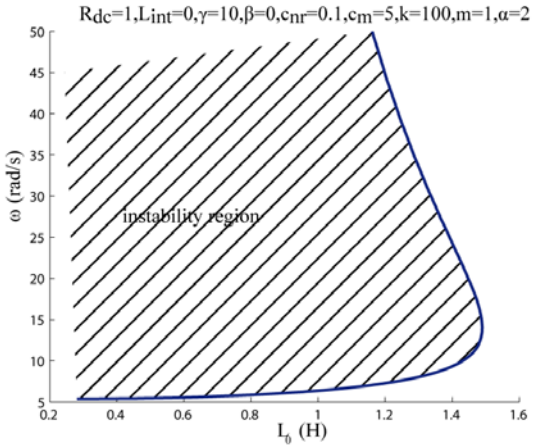

Figure 4: limit spin speed and instability region in function of the inductance for a given set of parameters for the electromechanical model

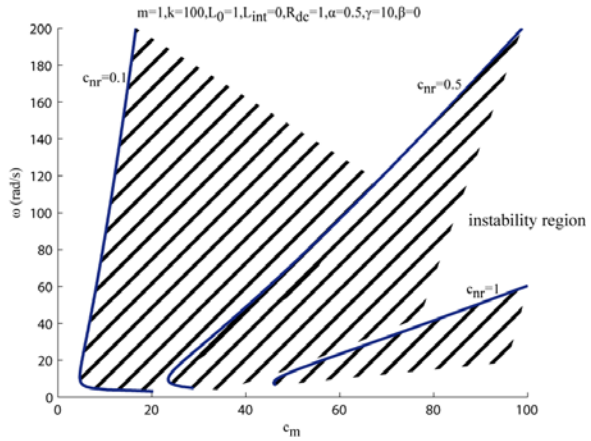

Figure 3: unstable speed range for a given set of parameters for the electromechanical model

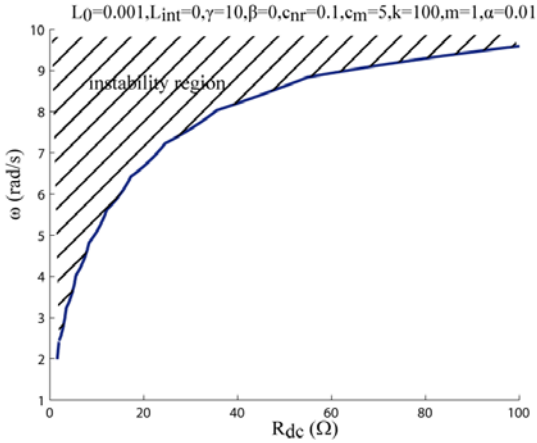

Figure 5: limit spin speed and instability region in function of the internal inductance for a given set of parameters for the electromechanical model

Concerning the roots of equation (6) however, it can be seen that they give a limited speed range where the behavior of the system is unstable. Indeed, the spin speed can go through a region where the system is unstable, and afterwards go into a region where the behavior is stable.

For instance, we can look at the instability region for a given set of parameters on figure 3. It is clear on this figure that the instability region has a finite limit. For instance, for a factor of proportion for the rotating damping c_m worth 10, and a non-rotating damping c_{nr} worth 0.1, the model predicts an unstable speed range from 4.16 rad/s to 86.85 rad/s. On this figure, it is also observable that when the non-rotating damping increases, the instabilty region shrinks.

We can further analyze the equations and see that obviously inductance is favorable to stability: on figure 4, we see that when the inductance increases, the instability region shrinks. When the inductance is high enough, there is no instability anymore. The interpretation of figure 5 is more complex: the weight low-frequency resistance decreases when the spin speed increases, and has no effect at high spin speed anymore.

V. APPLICATION

5.1. Magnetic bearing

The studied bearings (figures 1 and 6) have been developed to be used in a flywheel energy storage system [2]. It is thus important for its energy consumption to be minimum. They are semi-passive bearings. The axial axis is controlled actively. These bearings are used by pairs: the upper bearing pulls the flywheel up, acting against gravity, and the other one

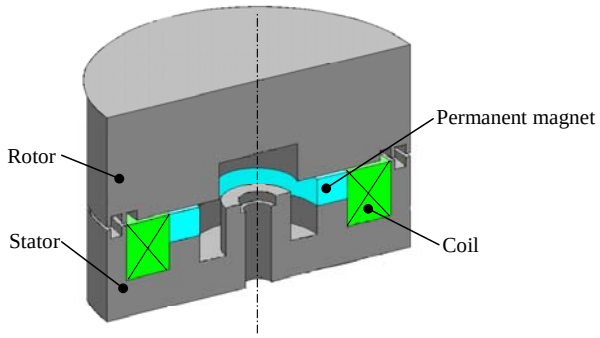

Figure 6: schematic drawing of lower semi-passive magnetic bearing

acts against the first one. The coils allow controlling the magnetic flux circulating inside the bearing, so to stabilize the system. At equilibrium, no current circulates inside the coils, and the position of the rotor is slightly closer to the upper bearing. The passive axis is the radial axis. The radial stiffness of the bearing is obtained through reluctance forces. The teeth at the periphery of the bearing produce that reluctant force.

5.2 Experimental setup

The experimental setup consists of a milling machine, a force sensor with strain gauges and one magnetic bearing.

The stator of the magnetic bearing is fixed to the machine frame via the force sensor. Indeed, by the action-reaction principle, the forces acting on the rotor of the magnetic bearing are equal but opposed to the forces measured on the stator. The milling machine allows a precise positioning of the rotating part of the bearing with respect to the fixed part. The milling machine can drive the rotor of the magnetic bearing to rotation speeds up to 6300 rpm.

VI. ELECTROMECHANICAL MODEL OF THE BEARING

6.1 Identification

In the electromechanical model, the parameters are unknown. First, an analysis of the physical phenomenon involved determines which parameters have to be taken into account, in the case of this semi-passive magnetic bearing. Then, the remaining parameters can be identified based on the experimental results for the forces exerted on the magnetic bearing.

First, to identify the stiffness coefficient intervening in the model, we measure the forces for different off-centred positions between the rotor and the stator when the rotating speed is zero. This stiffness is easily identified by a linear approximation. The average values of the stiffness in the x and in the y direction is worth 14024 N/m (Figure 7) for an air gap of 0.3 mm. Both stifnesses are a little different (13671 N/m, and 14378 N/m) due to a possible slight misalignment between the stator and the rotor when in centered position, and between the milling machine axis and the sensor axis.

Second, to identify the rotating damping and the impedance parameters, experiments have been made with the rotor fixed in an off-centred position (d = 0.5 mm), and the forces have been measured for various spin speed. In this case, according to the electromechanical model (10), the forces are worth:

$$F_x = -\frac{c_r(\omega)\omega}{\sqrt{1+(\omega L/R(\omega))^2}}d$$

$$F_y = -(k - \frac{c_r(\omega)\omega^2 L/R(\omega)}{\sqrt{1+(\omega L/R(\omega))^2}})d$$

The stiffness force can be considered as an offset not varying with the spin speed, and is subtracted to the experimental measurements. The other parameters can then be identified by the least square criterion.

The values of the parameters after identification are given in Table 1.

TABLE 1: value of the parameters for the magnetic bearing

c_m	0.32
L_0	$1.1472\ 10^{-4}$
L_{int}	0.0185
R_{dc}	$4.93\ 10^{-11}$
α	0.0135
γ	0.2278
β	$7.7421\ 10^{-12}$

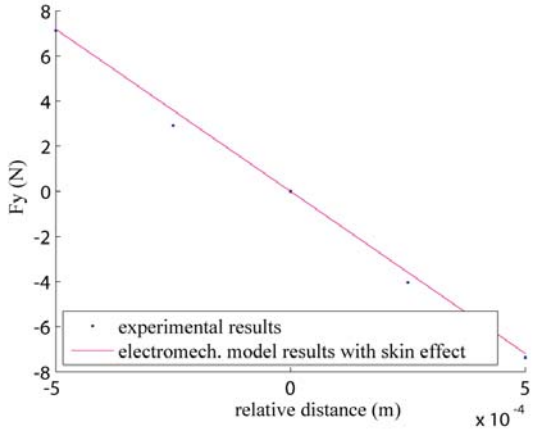

Figure 7: stiffness in the y direction of the magnetic bearing (air gap of 0.3 mm)

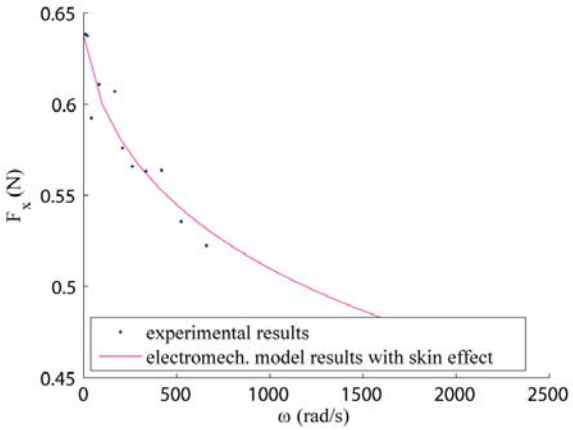

Figure 8: Experimental measurements and forces predicted by the parametrized electromechanical model for the force perpendicular to the relative displacement

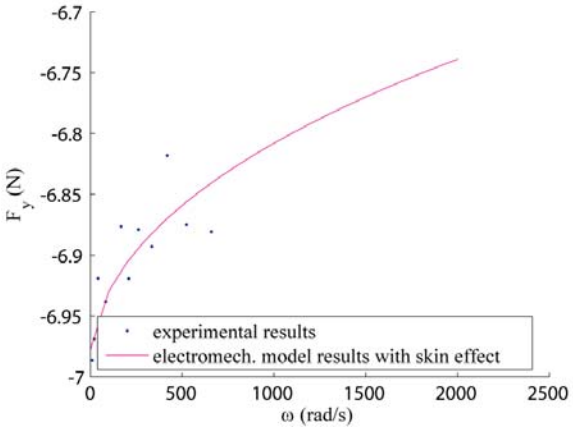

Figure 9: Experimental measurements and forces predicted by the parametrized electromechanical model for the force aligned on the relative displacement

Let's note that on Figure 8, F_x is not equal to zero for a spin speed equal to zero. This is due to the possible misalignment between the stator and the rotor when in centered position, and between the milling machine axis and the sensor axis. This offset has been subtracted to the force for the identification.

6.2 Comparison

It can be seen on Figure 8 and 9, that the parameter identification allows the electromechanical model to predict the measured forces very well. The evolution of the forces is respected on the whole speed range, and can predict the further evolution at higher spin speed.
These parameters have been identified for one off-centred position of 0.5 mm between the rotor and the stator, while they are supposing to vary with this position according to an evolution law that characterized a priori.

VII. CONCLUSION

A parametrical model has been presented representing the behavior of rotating systems submitted to electromagnetic forces, and especially forces due to the interaction of induced currents and magnetic fields. The electromagnetic forces were represented by mechanical componenets like springs and dampers. The inductive and resistive effects were taken into account by introducing a phase shift and a variable damping coefficient. The skin effect was also taken into account by allowing the resistive and inductive effects to vary with the spin speed. The parameters of the electromechanical model were easily identified, and show a good concordance between the forces measured on the bearing, and the forces predicted by the electromechanical model.

This study should be completed by a finite element study of the electromagnetic bearing, but it can already be concluded that the assumptions on which the model are based are valid.

The approach proposed via this electromechanical model allows to design or to work on existing bearings, and to predict their behavior without knowing the exact magnetic and electric field distribution.

VIII. REFERENCES

1. Xu Yanliang, Dun Yueqin, Wang Xiuhe, Kong yu, Analysis of hybrid magnetic bearing with a permanent magnet in the rotor by FEM, IEEE Trans. on magnetics, volume 42, n°4**,** pp1363-1366
2. F. Faure, Magnetic suspension for flywheels (in French), Ph. D. thesis, INP Grenoble (2003)
3. V. Kluyskens, B. Dehez, H. Ben Ahmed, Dynamical electromechanical model for magnetic bearings, IEEE Trans. on magnetics, volume 43, no7, pp3287-3292 (july 2007)
4. G. Genta, Vibration of structures and machines, 3rd ed., New York, Springer, 1999
5. V. Kluyskens, B. Dehez, Comparison between models predicting the evolution of the electrical impedance with frequency, submitted to Compel